

$^{116}\text{Sn}(^{58}\text{Ni},\text{p}2\text{n}\gamma)$ **1999Ba84**

Type	Author	History	Citation	Literature Cutoff Date
Full Evaluation	Coral M. Baglin, E. A. Mccutchan		NDS 151, 334 (2018)	30-Jun-2018

1999Ba84: E=260 MeV, PEX array (4 Compton-suppressed Euroball cluster detectors and Si-ball with 32 elements); E=267 MeV, JUROSPHERE array (25 Compton suppressed Ge detectors, 10 TESSA detectors at 79° and 101°, 15 EUROGAM detectors at 134° and 158°); RITU recoil separator for α decay tagging of gammas; measured $E\gamma$, $\gamma\gamma$ coin, $I\gamma$, (recoil)- γ coin, (recoil)- $\gamma\gamma$ coin, $\gamma(\theta)$.

 ^{171}Ir Levels

E(level) [†]	J ^π [‡]	Comments
0.0+x [@]	11/2 ⁻	
436.04+x [#] 4	13/2 ⁻	
633.90+x [@] 4	15/2 ⁻	
997.82+x ¹⁶		
1115.95+x [#] 5	17/2 ⁻	
1353.07+x [@] 7	19/2 ⁻	
1365.77+x ^d 8	17/2 ⁻	
1520.70+x ²³		
1609.30+x ^d 6	19/2 ⁻	
1823.44+x [#] 11	21/2 ⁻	
1884.61+x ^d 7	21/2 ⁻	
2008.47+x ^a 12	(21/2)	
2106.40+x [@] 13	23/2 ⁻	
2326.71+x ^{&} 15	(23/2 ⁻)	
2334.14+x ^a 15	(23/2)	
2335.5+x ¹⁰		
2381.49+x ^{&} 10	(25/2 ⁻)	
2444.88+x [#] 16	25/2 ⁻	
2496.75+x ^{&} 11	(27/2 ⁻)	
2589.7+x ^e 3		
2677.89+x ^{&} 12	(29/2 ⁻)	
2690.44+x ²⁵	(25/2)	
2705.16+x ^a 23	(25/2)	
2730.87+x [@] 21	27/2 ⁻	
2796.9+x ^e 4		
2945.56+x ^{&} 13	(31/2 ⁻)	
3096.0+x ^e 4		
3284.17+x ^{&} 15	(33/2 ⁻)	
3631.70+x ^{&} 19	(35/2 ⁻)	
0.0+y ^b	(23/2)	E(level): level decays to 1353+x (19/2 ⁻) and 1116+x (17/2 ⁻) levels via unidentified linking transitions; so y>1353.
98.00+y ^b 15	(25/2 ⁻)	
223.00+y ^b 20	(27/2)	
424.18+y ^b 22	(29/2)	
670.97+y ^b 24	(31/2)	
955.8+y ^b 3	(33/2)	
1275.2+y ^b 3	(35/2)	
1631.0+y ^b 5	(37/2)	

Continued on next page (footnotes at end of table)

$^{116}\text{Sn}(^{58}\text{Ni},\text{p}2\text{n}\gamma)$ **1999Ba84 (continued)** ^{171}Ir Levels (continued)

E(level) [†]	J ^π [‡]	Comments
0.0+z ^c	(9/2 ⁻)	E(level): This level feeds the 1253, 19/2 ⁻ and 1176, 17/2 ⁻ levels, so z>1253.
300.59+z ^c 6	(13/2 ⁻)	
774.50+z ^c 10	(17/2 ⁻)	
1361.65+z ^c 15	(21/2 ⁻)	
1972.15+z ^c 21	(25/2 ⁻)	
2623.7+z ^c 3	(29/2 ⁻)	

[†] From least-squares fit to E_γ.

[‡] Authors' values based on transition multipolarities, deduced band structure, population strengths and comparison with band structure in heavier Ir isotopes.

Band(A): πh_{11/2}, α=+1/2 band. Proton probably coupled to triaxially deformed core; band probably crossed at high spin by prolate 3-quasiparticle structure.

@ Band(a): πh_{11/2}, α=-1/2 band. See comment on signature partner of this band.

& Band(B): π=-, ΔJ=1 band. Lowest-energy level feeds (21/2⁻) state. Possible configuration=(πh_{11/2})(v_{13/2})².

^a Band(C): ΔJ=1 3-quasiparticle band. Lowest-energy level feeds (19/2⁻) g.s. band member.

^b Band(D): ΔJ=1 3-quasiparticle band. Lowest-energy level feeds (17/2⁻) and (19/2⁻) g.s. band members. Possible configuration=(πh_{11/2})(v²).

^c Band(E): Possible πh_{9/2} band. Assignment of band to ¹⁷¹Ir is tentative because α tagging spectrum is ambiguous; 301γ and 610γ may be strongly contaminated in that spectrum.

^d Band(F): π=- band fragment. Lowest-energy level feeds (13/2⁻) g.s. band member.

^e Band(G): Band fragment. Lowest-energy level feeds (21/2⁻) state.

 $\gamma(^{171}\text{Ir})$

E _γ	I _γ	E _i (level)	J _i ^π	E _f	J _f ^π	Comments
98.00 15		98.00+y	(25/2 ⁻)	0.0+y	(23/2)	
115.26 6	4.2 3	2496.75+x	(27/2 ⁻)	2381.49+x	(25/2 ⁻)	
125.00 12	4.3 4	223.00+y	(27/2)	98.00+y	(25/2 ⁻)	
181.14 5	9.4 4	2677.89+x	(29/2 ⁻)	2496.75+x	(27/2 ⁻)	
197.65 5	15.8 10	633.90+x	15/2 ⁻	436.04+x	13/2 ⁻	E _γ : fits this placement very poorly.
201.18 10	5.8 5	424.18+y	(29/2)	223.00+y	(27/2)	
207.20 11	3.3 3	2796.9+x		2589.7+x		
236.96 11	7.1 6	1353.07+x	19/2 ⁻	1115.95+x	17/2 ⁻	
243.55 6	10.5 5	1609.30+x	19/2 ⁻	1365.77+x	17/2 ⁻	A ₂ =+0.05 10; consistent with D+Q transition.
246.79 10	5.9 4	670.97+y	(31/2)	424.18+y	(29/2)	
256.31 10	6.4 5	1609.30+x	19/2 ⁻	1353.07+x	19/2 ⁻	
267.67 5	10.8 5	2945.56+x	(31/2 ⁻)	2677.89+x	(29/2 ⁻)	
275.31 4	60.4 21	1884.61+x	21/2 ⁻	1609.30+x	19/2 ⁻	A ₂ =+0.07 5; consistent with D+Q transition.
282.83 16	5.5 6	2106.40+x	23/2 ⁻	1823.44+x	21/2 ⁻	
284.82 13	5.0 5	955.8+y	(33/2)	670.97+y	(31/2)	
285.98 15	<7.8	2730.87+x	27/2 ⁻	2444.88+x	25/2 ⁻	
299.06 16	3.0 3	3096.0+x		2796.9+x		
300.59 6	>17.7	300.59+z	(13/2 ⁻)	0.0+z	(9/2 ⁻)	
319.45 14	4.3 4	1275.2+y	(35/2)	955.8+y	(33/2)	
325.67 9	8.8 6	2334.14+x	(23/2)	2008.47+x	(21/2)	
338.42 12	7.6 7	2444.88+x	25/2 ⁻	2106.40+x	23/2 ⁻	
338.61 7	6.9 4	3284.17+x	(33/2 ⁻)	2945.56+x	(31/2 ⁻)	
347.53 11	3.9 3	3631.70+x	(35/2 ⁻)	3284.17+x	(33/2 ⁻)	
355.8 3	1.5 3	1631.0+y	(37/2)	1275.2+y	(35/2)	

Continued on next page (footnotes at end of table)

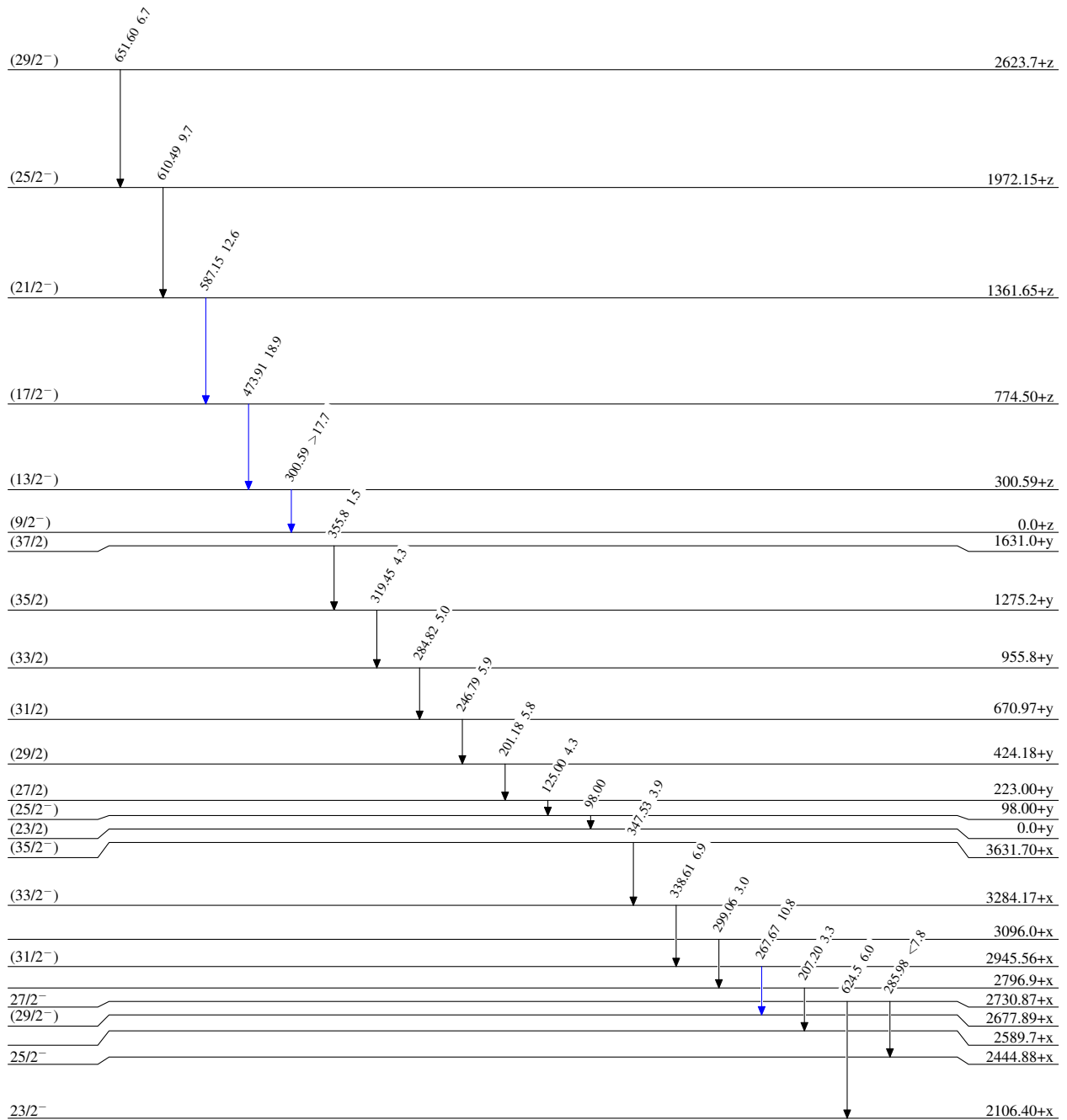
$^{116}\text{Sn}(^{58}\text{Ni},\text{p}2\text{n}\gamma)$ **1999Ba84** (continued) $\gamma(^{171}\text{Ir})$ (continued)

E_γ	I_γ	$E_i(\text{level})$	J_i^π	E_f	J_f^π	Mult.	Comments
356.30 19	3.2 4	2690.44+x	(25/2)	2334.14+x	(23/2)		
371.02 17	4.3 5	2705.16+x	(25/2)	2334.14+x	(23/2)		
435.97 4	46.1 25	436.04+x	13/2 ⁻	0.0+x	11/2 ⁻		$A_2=+0.25$ 3.
442.10 13	8.4 7	2326.71+x	(23/2 ⁻)	1884.61+x	21/2 ⁻		
470.49 14	11.2 10	1823.44+x	21/2 ⁻	1353.07+x	19/2 ⁻		
473.91 8	18.9 12	774.50+z	(17/2 ⁻)	300.59+z	(13/2 ⁻)		
481.94 4	63 3	1115.95+x	17/2 ⁻	633.90+x	15/2 ⁻		
493.32 4	53.9 21	1609.30+x	19/2 ⁻	1115.95+x	17/2 ⁻		$A_2=0.00$ 6; consistent with D+Q transition.
496.88 6	30.6 13	2381.49+x	(25/2 ⁻)	1884.61+x	21/2 ⁻		
522.88 17	10.7 10	1520.70+x		997.82+x			
531 3	0.6 8	1884.61+x	21/2 ⁻	1353.07+x	19/2 ⁻		
561.78 15	14.6 15	997.82+x		436.04+x	13/2 ⁻		
587.15 11	12.6 9	1361.65+z	(21/2 ⁻)	774.50+z	(17/2 ⁻)		
610.49 14	9.7 7	1972.15+z	(25/2 ⁻)	1361.65+z	(21/2 ⁻)		
621.63 22	10.9 12	2444.88+x	25/2 ⁻	1823.44+x	21/2 ⁻		
624.5 4	6.0 10	2730.87+x	27/2 ⁻	2106.40+x	23/2 ⁻		
634.00 5	101 8	633.90+x	15/2 ⁻	0.0+x	11/2 ⁻	Q	Mult.: $A_2=+0.32$ 4.
651.60 19	6.7 6	2623.7+z	(29/2 ⁻)	1972.15+z	(25/2 ⁻)		
655.39 10	25.2 16	2008.47+x	(21/2)	1353.07+x	19/2 ⁻		
680.09 7	34.8 17	1115.95+x	17/2 ⁻	436.04+x	13/2 ⁻	Q	Mult.: $A_2=+0.26$ 6.
705.1 3	2.6 7	2589.7+x		1884.61+x	21/2 ⁻		
707.24 18	14.7 13	1823.44+x	21/2 ⁻	1115.95+x	17/2 ⁻		
719.32 7	65 3	1353.07+x	19/2 ⁻	633.90+x	15/2 ⁻	Q	Mult.: $A_2=+0.37$ 4.
753.35 14	18.3 13	2106.40+x	23/2 ⁻	1353.07+x	19/2 ⁻		
929.83 12	14.8 15	1365.77+x	17/2 ⁻	436.04+x	13/2 ⁻		
982.4 10	3.1 11	2335.5+x		1353.07+x	19/2 ⁻		

$^{116}\text{Sn}(^{58}\text{Ni},\text{p}2\text{n}\gamma)$ 1999Ba84Level Scheme
Intensities: Relative I_γ

Legend

- $I_\gamma < 2\% \times I_\gamma^{\text{max}}$
- $I_\gamma < 10\% \times I_\gamma^{\text{max}}$
- $I_\gamma > 10\% \times I_\gamma^{\text{max}}$

 $^{171}_{77}\text{Ir}_{94}$

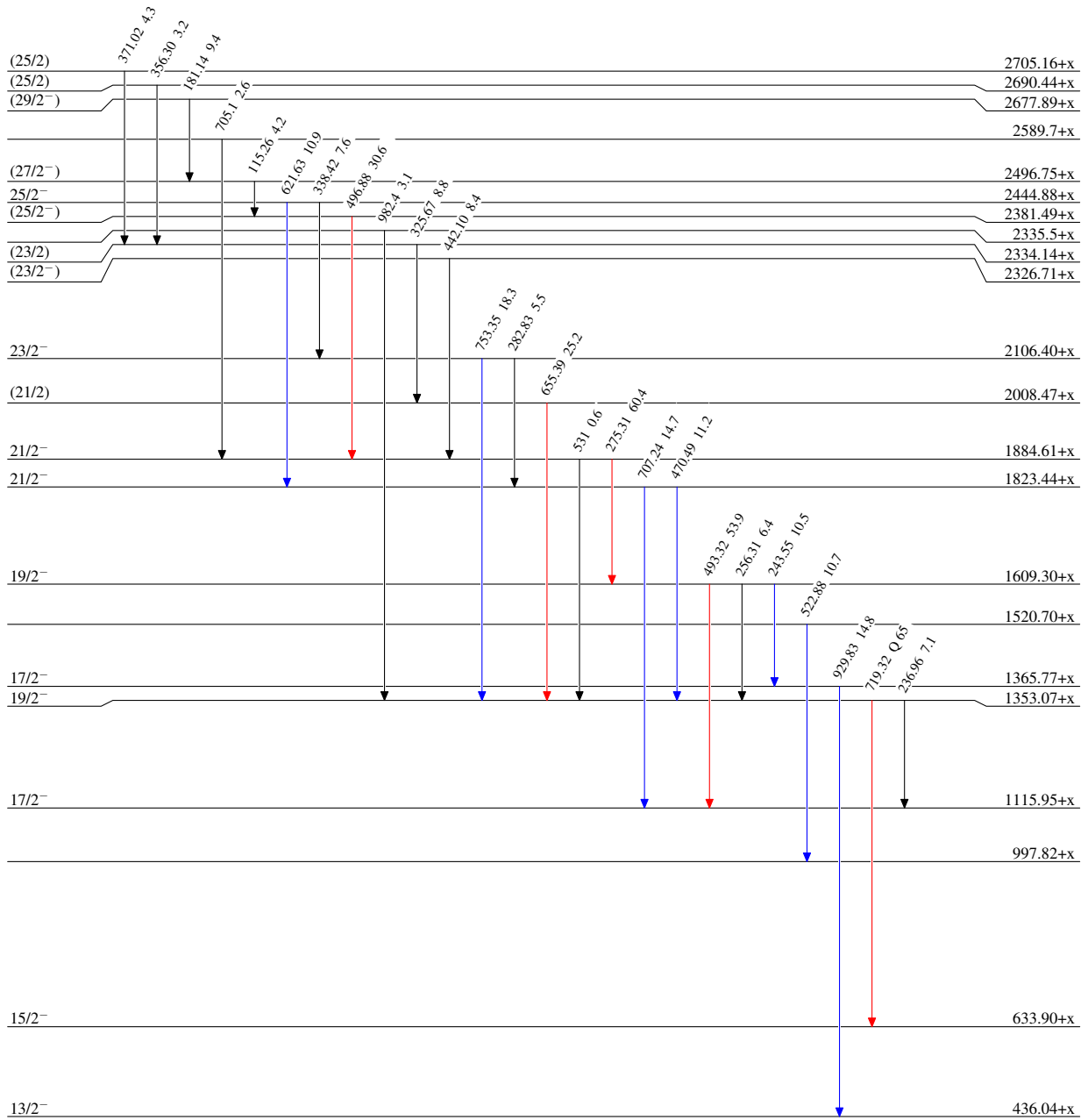
$^{116}\text{Sn}(^{58}\text{Ni},\text{p}2\text{n}\gamma) \quad 1999\text{Ba}84$

Level Scheme (continued)

Intensities: Relative I_γ

Legend

- $I_\gamma < 2\% \times I_\gamma^{\text{max}}$
- $I_\gamma < 10\% \times I_\gamma^{\text{max}}$
- $I_\gamma > 10\% \times I_\gamma^{\text{max}}$

 $^{171}_{77}\text{Ir}_{94}$

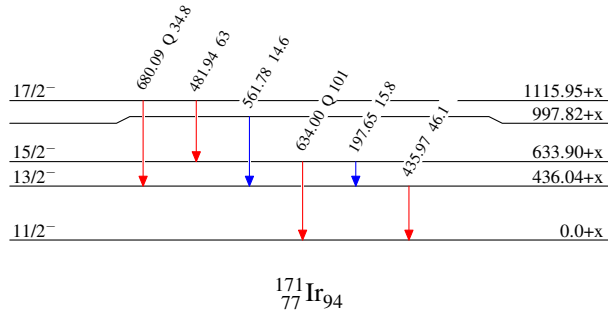
$^{116}\text{Sn}(^{58}\text{Ni},p2n\gamma)$ 1999Ba84

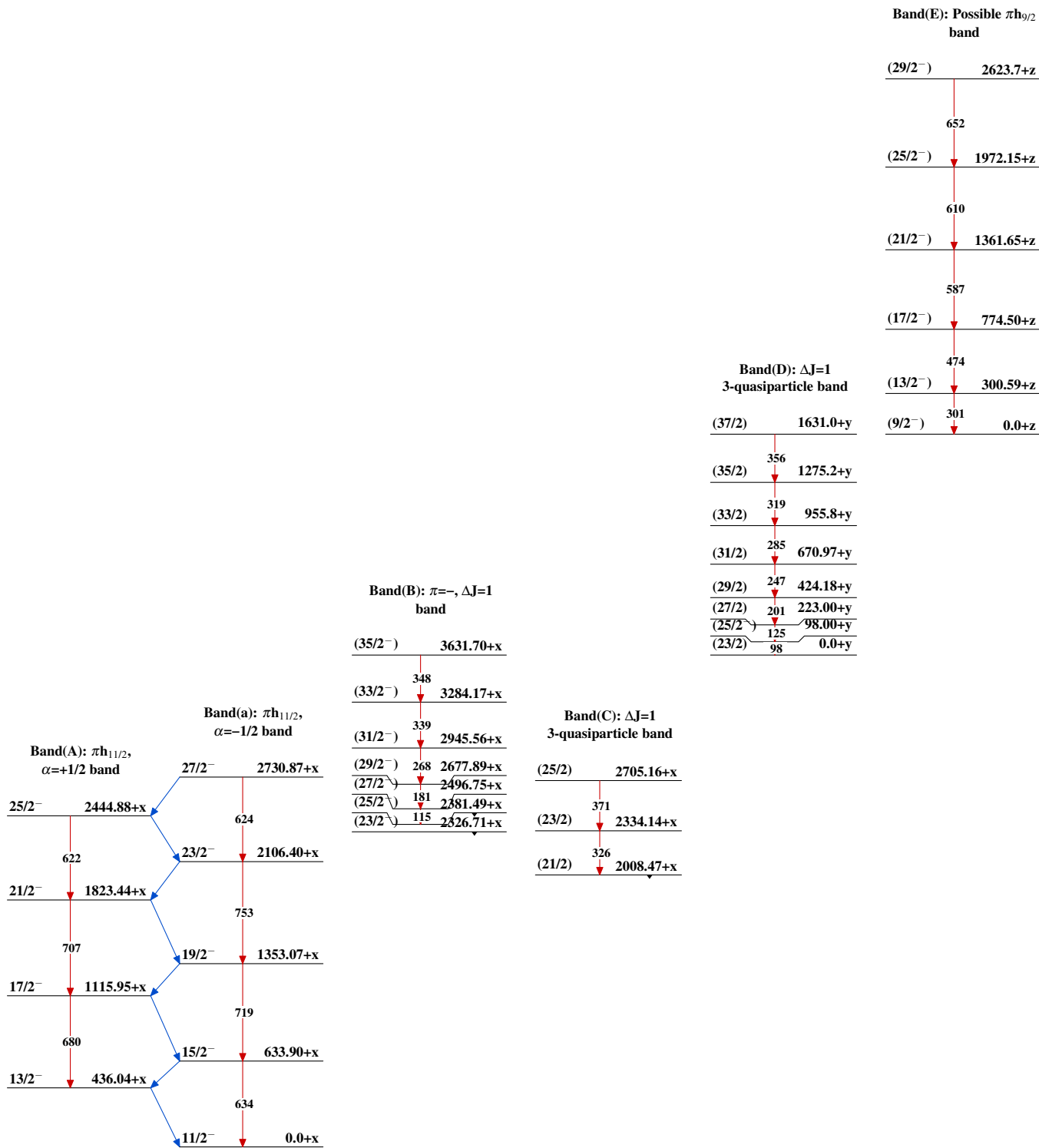
Level Scheme (continued)

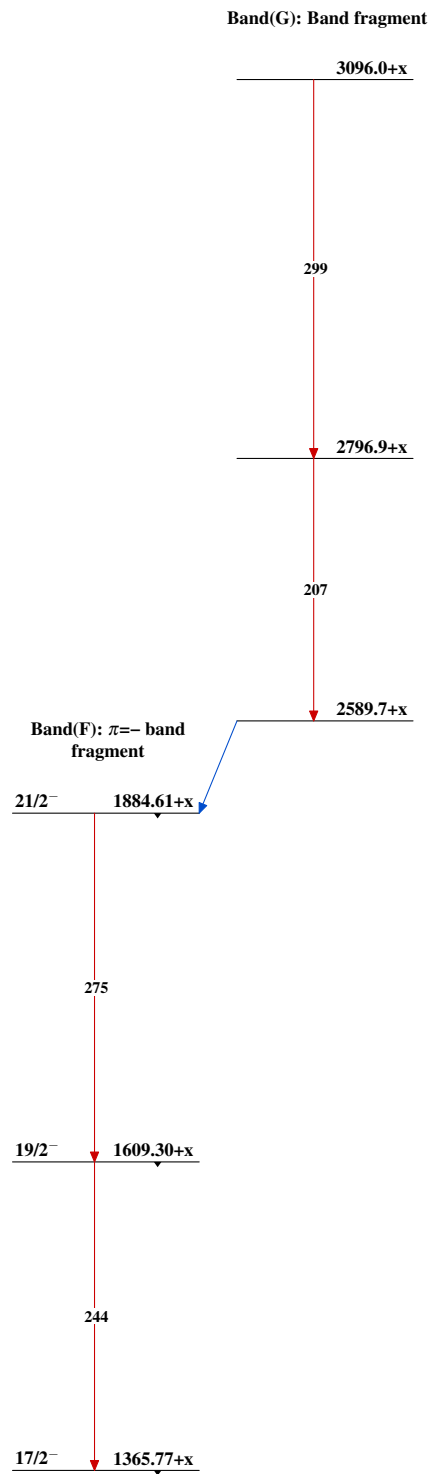
Intensities: Relative I_γ

Legend

- $I_\gamma < 2\% \times I_\gamma^{\text{max}}$
- $I_\gamma < 10\% \times I_\gamma^{\text{max}}$
- $I_\gamma > 10\% \times I_\gamma^{\text{max}}$



$^{116}\text{Sn}(^{58}\text{Ni},p2n\gamma)$ 1999Ba84

$^{116}\text{Sn}(^{58}\text{Ni},\text{p}2\text{n}\gamma)$ 1999Ba84 (continued) $^{171}_{77}\text{Ir}_{94}$